Inorganic Chemistry

pubs.acs.org/IC Article

Visible Light Absorption and Long-Lived Excited States in Dinuclear Silver(I) Complexes with Redox-Active Ligands

Dylan J. Shields, Tasneem Elkoush, Emily Miura-Stempel, Choi L. Mak, Guang-Hao Niu, Anna D. Gudmundsdottir, and Michael G. Campbell*

Cite This: *Inorg. Chem.* 2020, 59, 18338−18344 Read Online

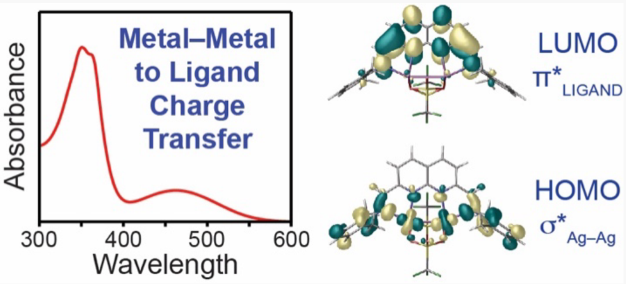

ABSTRACT: Well-defined dinuclear silver(I) complexes have been targeted for applications in catalysis and materials chemistry, and the effect of close silver−silver interactions on electronic structure remains an area of active inquiry. In this study, we describe the synthesis, structure, and photophysical properties of dimeric silver complexes featuring a redox-active naphthyridine diimine ligand. Unusually for silver(I), these complexes display absorption features in the visible region due to metal−metal to ligand charge transfer (MMLCT) transitions, which arise from the combination of close silver−silver interactions and low-lying ligand π^* orbitals. The complexes' photophysical properties are explored via a combination of spectroscopic and computational studies, revealing MMLCT excited state lifetimes that exceed 1 μs. These results portend previously unforeseen applications of silver(I) dimers in visible light absorption and excited state reactivity.

■ INTRODUCTION

Multinuclear silver complexes featuring silver−silver interactions have long been of interest for varied areas including catalysis, supramolecular chemistry, and optical and electronic materials.[1−4] And while "argentophilic" interactions between closed-shell d^{10} silver(I) centers have been recognized since the 1980s,[5] they are in general still poorly understood. A recent comprehensive review on the subject notes the "paucity of data from criteria other than the Ag−Ag distance...[from] which to draw conclusions" about bonding in such complexes.[6] In part, this is due to the wide-ranging and often unpredictable coordination chemistry of silver(I), which makes it challenging to apply the classical theoretical paradigm of metal−metal bonding to silver in a general way.[7] As part of our research program on better understanding the chemistry of dinuclear silver complexes,[8] our group has been interested in synthesizing structurally well-defined silver(I) dimers that feature close silver−silver interactions, and investigating their electronic structures.

A recent area of interest for dimeric transition metal complexes has been their visible light photochemistry. As compared to monomeric complexes that have traditionally been used for such applications (e.g., the archetypal Ru$(bpy)_3Cl_2$ and its many analogues),[9] it has been found that metal−metal interactions provide an additional handle for tuning photophysical properties such as absorption wavelength, excited state lifetime, and excited state redox potentials. Metal dimers have therefore begun to receive significant attention for applications in light harvesting, photo-induced electron transfer reactions, and photoredox catalysis.[10] A drawback, however, is that the systems reported to date are generally based on expensive precious metal dimers such as rhodium or platinum.

Unsurprisingly, silver has not previously been viewed as a promising candidate for applications in photochemistry with visible light. Silver(I) complexes, with d^{10} electronic configurations, are typically colorless, and higher oxidation state complexes of silver with partially filled *d* shells generally exhibit poor stability that precludes their use in such applications. In this report, we describe two new dimeric silver(I) complexes that feature a redox-active naphthyridine-based ligand, which display unusual absorption features in the visible region. The electronic structure of the complexes is probed through a combination of spectroscopic and computational studies, revealing long-lived metal−metal to ligand charge transfer (MMLCT) excited states. Our results open up new areas of exploration for silver(I) in visible light photochemistry.

■ RESULTS AND DISCUSSION

Synthesis and Structural Characterization. Naphthyridine-based scaffolds are a privileged family of ligands that have

Received: October 2, 2020
Published: December 9, 2020

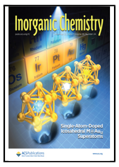

been used to produce a wide array of dinuclear metal complexes.[11] A handful of dimeric silver(I) complexes have also been structurally characterized using simple naphthyridine ligands.[12] We have recently been working to expand the range of silver−naphthyridine coordination chemistry, and our preliminary efforts in this area have shown that strictly limiting ligand flexibility is critical to obtaining the desired dincluear complexes, as opposed to coordination polymers that exhibit fluxional behavior in solution.[13] In this study, we targeted the naphthyridine diimine (NDI) ligand ^{i}PrNDI (**1**, Figure 1). Closely related ligands have recently been used by the Uyeda group for redox catalysis with dinuclear nickel complexes,[14] as well as by others for dinuclear complexes with metals such as copper and ruthenium.[15]

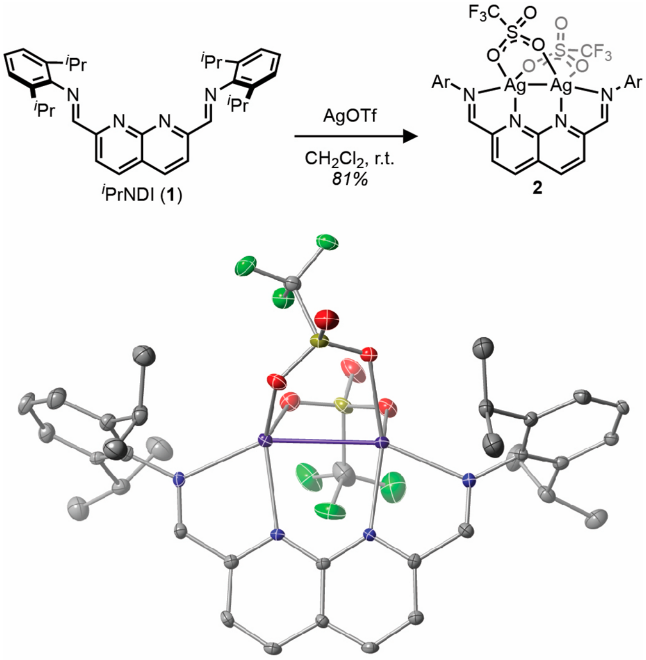

Figure 1. Synthesis and crystal structure of silver dimer **2**, with a close Ag−Ag distance of 2.9179(5) Å (structure plotted with 50% probability ellipsoids, H atoms and solvent molecules omitted for clarity).

Combining ligand **1** with 2 equiv of AgOTf in CH_2Cl_2 at room temperature produced a color change from pale yellow to orange, followed by further development of a deeper cherry red color. Diffusion of Et_2O into the reaction mixture produced red/orange crystals in 81% isolated yield, and single-crystal X-ray diffraction (SCXRD) analysis revealed dinuclear complex **2** (Figure 1). The silver centers in **2** exhibit a close silver−silver distance of 2.9179(5) Å, well below the sum of the van der Waals radii (∼3.44 Å),[6] and are bridged by the two triflate anions in addition to the ^{i}PrNDI ligand. In CD_2Cl_2, **2** displays a ^{1}H NMR spectrum consistent with the approximate C_{2v} symmetry of the solid-state structure (Figure S13), and persistence of the dinuclear structure of **2** in solution is also supported by HRMS analysis (Figure S8).

Our observations indicate that the initial orange color observed upon combining **1** and AgOTf, prior to formation of the darker red color of **2**, is due to the formation of mono-metalated products. If Et_2O diffusion into the reaction mixture is carried out immediately after the ligand and metal salt are combined, pale yellow/orange crystals of the mononuclear complex $[(^{i}PrNDI)_2Ag][OTf]$ (**3**) are obtained (Figure 2). SCXRD analysis shows that the silver center is ligated by one naphthyridine nitrogen atom and one imine from each ^{i}PrNDI ligand, with distortions from an idealized tetrahedral geometry caused by steric repulsion between the two bulky ligands. Complex **3** could also be independently synthesized by combining a 2:1 ratio of **1** and AgOTf in MeCN; full details of the synthesis and characterization are described in the Supporting Information.

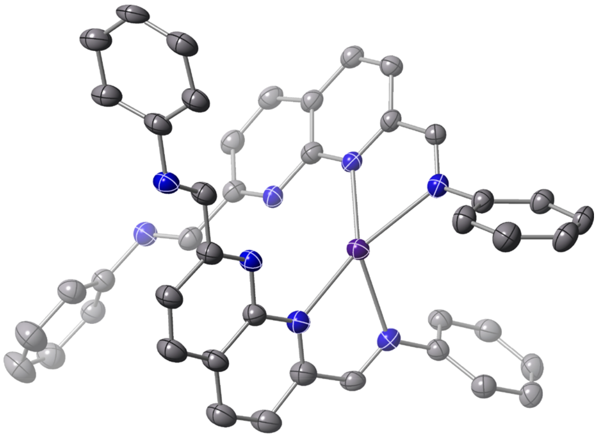

Figure 2. X-ray structure of the cation of mononuclear silver complex $[(^{i}PrNDI)_2Ag][OTf]$ (**3**), formed on path to dinuclear complex **2** (50% probability ellipsoids, H atoms and isopropyl groups omitted for clarity).

We find that the bridging triflate anions of **2** are extremely labile. Exposure to ambient atmosphere, or intentional introduction of water or Lewis basic solvents such as MeCN, results in rapid ligand scrambling. Recrystallization of **2** from either wet CH_2Cl_2 solutions or MeCN solutions produced red/orange crystals of the new dinuclear complex $[(^{i}PrNDI)_2Ag_2][OTf]_2$ (**4·OTf**, Figure 3). Surprisingly, despite their rigidity and steric bulk, two ^{i}PrNDI ligands bridge two silver centers in **4**. A related structure has previously been reported for copper(I), using an NDI ligand with less bulky substituents on the imine aryl rings.[15a] The silver atoms in **4** are distorted away from the plane defined by either naphthyridine group, resulting in a slightly elongated silver−silver distance compared to **2**, 3.0095(5) Å.

^{1}H NMR analysis shows that, in CD_2Cl_2 solutions of **2** that are not rigorously dry, **2** and **4** are in equilibrium, leading to broad resonances for the ^{i}PrNDI ligand at room temperature. At lower temperatures, the spectrum resolves into two sets of well-defined signals corresponding to **2** and **4** (Figure S22). Attempts to independently prepare **4·OTf** by combining a 1:1 ratio of **1** and AgOTf in CH_2Cl_2 resulted in similar solution-phase behavior, again suggesting an equilibrium between **2** and **4**. To avoid this dynamic behavior and to fully characterize complex **4**, we replaced the triflate anions with more weakly coordinating hexafluorophosphate anions, and the resulting product **4·PF$_6$** was obtained in 90% isolated yield after recrystallization from CH_2Cl_2/Et_2O. Complex **4·PF$_6$** is deep cherry red in CH_2Cl_2 solutions and displays sharp and well-defined ^{1}H NMR signals (Figure S19); the solution-phase structure is further supported by HRMS analysis (Figure S10). SCXRD analysis indicates that the counteranion has a negligible effect on the solid-state structure of **4**, and similar structural metrics were observed between crystals of **4** with

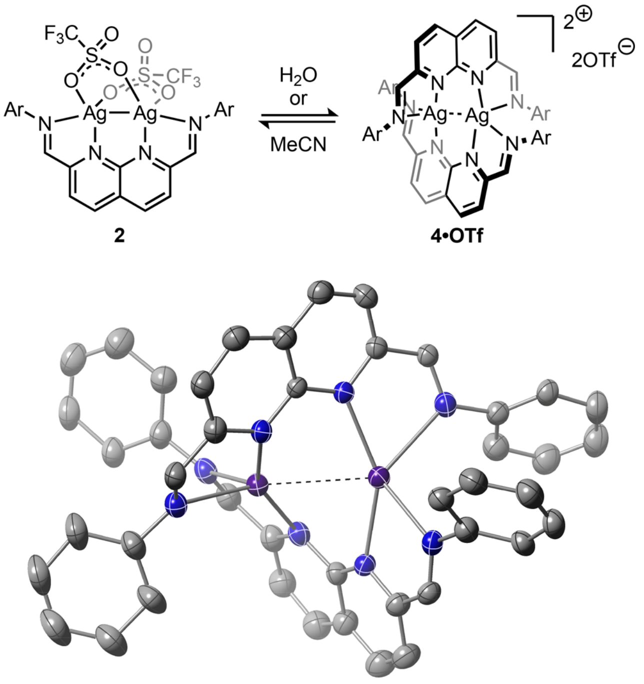

Figure 3. The presence of water or Lewis basic solvents leads to dynamic ligand exchange, and an equilibrium between **2** and $[(^{i}\mathrm{PrNDI})_2\mathrm{Ag}_2][\mathrm{OTf}]_2$ (**4·OTf**) (X-ray structure of the cation of **4** plotted with 50% probability ellipsoids, H atoms and isopropyl groups omitted for clarity).

triflate or hexafluorophosphate anions. Crystals of **4·PF$_6$** contain two crystallographically independent molecules of **4**, with silver−silver distances of 3.0552(6) and 3.0563(7) Å (Figure S4).

Electronic Structure. One of the most immediately interesting characteristics of complexes **2** and **4** is their deep red color, which is highly unusual for silver(I) complexes that lack possible *d*−*d* transitions. UV−vis spectra of **2** and **4·PF$_6$** in CH_2Cl_2 both display similar features (Figure 4): complex **2** exhibits features with λ_{max} = 257 nm ($\varepsilon = 2.3 \times 10^4$ M^{-1} cm^{-1}), 351 nm ($\varepsilon = 9.7 \times 10^3$ M^{-1} cm^{-1}), 364 nm ($\varepsilon = 9.5 \times 10^3$ M^{-1} cm^{-1}), and 467 nm ($\varepsilon = 1.8 \times 10^3$ M^{-1} cm^{-1}); complex **4** exhibits features with λ_{max} = 254 nm ($\varepsilon = 4.7 \times 10^4$ M^{-1} cm^{-1}), 348 nm ($\varepsilon = 1.9 \times 10^4$ M^{-1} cm^{-1}), and 460 nm ($\varepsilon = 4.8 \times 10^3$ M^{-1} cm^{-1}). For comparison, the ^{i}PrNDI ligand itself is pale yellow, with absorption maxima at λ = 252 nm ($\varepsilon = 4.3 \times 10^4$ M^{-1} cm^{-1}), 331 nm ($\varepsilon = 8.3 \times 10^3$ M^{-1} cm^{-1}), 345 nm ($\varepsilon = 9.2 \times 10^3$ M^{-1} cm^{-1}), and a broad shoulder that stretches from approximately 350 to 450 nm.

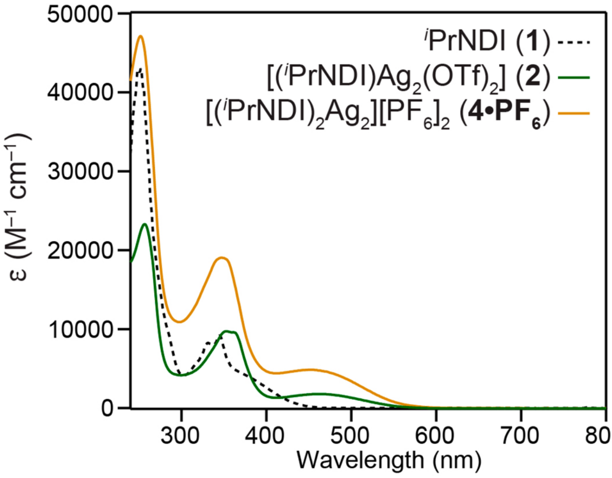

Figure 4. UV−vis spectra for complexes **2** and **4·PF$_6$** in CH_2Cl_2, overlaid with the spectrum of ligand **1**.

In contrast to dimeric complexes **2** and **4**, mononuclear complex **3** is yellow in color and displays a UV−vis spectrum with features essentially identical to those of ligand **1** (Figure S5). Similar to what we observe here for complex **3**, related mononuclear silver complexes with pyridine diimine ligands are also yellow in color and do not display any unusual low-energy absorption features.[16] Furthermore, to the best of our knowledge there is no recognized trend of close silver−silver interactions resulting in new low-energy electronic transitions, among the wide library of known multinuclear silver(I) complexes. The closest point of comparison is an elegant study from Che and co-workers, demonstrating that close interactions between silver(I) centers can produce 4dσ^*→5pσ transitions in the UV region.[3c] We therefore expected that the absorption features of **2** and **4** result from a combination of the disilver core and the redox-active ^{i}PrNDI ligand.

Time-dependent density functional theory (TD-DFT) calculations were performed on the geometry-optimized structures of complexes **2** and **4**. Analysis of the molecular orbitals (MOs) involved in the observed electronic transitions shows that the absorption features of **2** and **4** in the visible region have MMLCT character (Figure 5). For both complexes, the lowest unoccupied MOs are π^* orbitals of the ^{i}PrNDI ligand, whereas the *d* orbitals of the silver−silver core contribute significantly to the occupied frontier MOs. For comparison, TD-DFT calculations on ^{i}PrNDI ligand **1** indicate that its yellow color is mainly due to the HOMO→LUMO transition, in which the HOMO is localized on the pendant arylimines and the LUMO is localized on the central NDI π-system (Table S6). Such intraligand transitions also contribute to the absorption features of **2** and **4**, but do not account for the significantly increased absorption at longer wavelengths as compared to **1**.

For complex **2**, the HOMO has clear $\sigma^*_{\mathrm{Ag-Ag}}$ character, while the HOMO−1 has slight bonding overlap between the silver centers. The HOMO−6 is also antibonding with respect to the silver−silver interaction, and a $\sigma_{\mathrm{Ag-Ag}}$ bonding orbital is located at HOMO−9. Transitions between these occupied MOs and the ligand-based LUMO and LUMO+1 are the primary contributors to the observed absorption features at both 364 and 467 nm (Figure 5, left; Table S9). Further analysis of the frontier MOs of **2**, including atomic compositions of the relevant MOs, is given in Table S8 of the Supporting Information.

In complex **4**, the silver centers are less rigidly held in close contact as compared to **2**, which is reflected in the calculated frontier MOs (Figure 5, right). The ligand-based LUMO and LUMO+1 are found to be effectively degenerate; similarly, the HOMO through HOMO−3 are energetically very closely spaced and feature a mix of antibonding and nonbonding orbital interactions with respect to the two silver centers. Both the HOMO−1 and HOMO−8 feature antibonding interactions between the silver d_z2 orbitals, and a corresponding bonding combination is located at HOMO−10. TD-DFT calculations indicate that these orbitals are primary contributors to the transitions observed at 348 and 460 nm, along with the HOMO−11, which is effectively nonbonding with

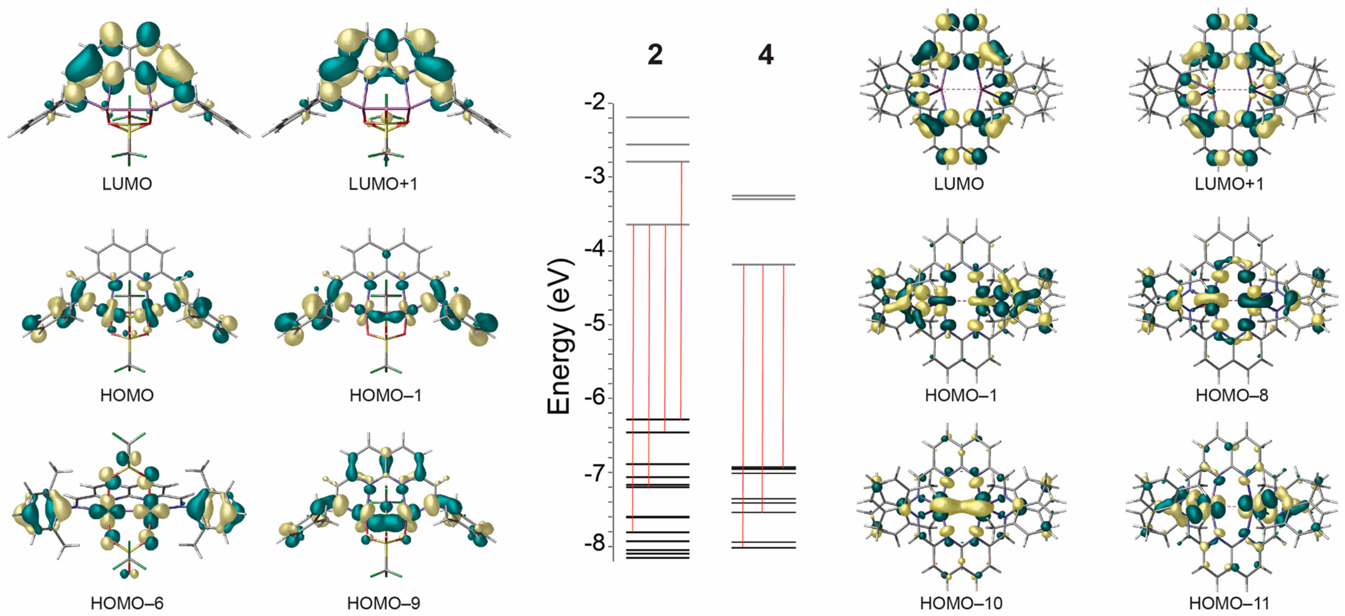

Figure 5. DFT-calculated molecular orbital (MO) diagrams for **2** and **4**, showing electronic transitions that are primary contributors to the observed absorption features in the visible region, along with visualizations of selected MOs with relevance to MMLCT transitions (details of DFT calculations given in the Supporting Information).

respect to the silver–silver interaction (Table S14). Further orbital analysis for complex **4** can also be found in Table S13.

For comparison, DFT calculations were also performed on mononuclear complex **3** (Tables S10 and S11). In contrast to dimeric complexes **2** and **4**, both the occupied and unoccupied frontier MOs of **3** are found to be almost entirely ligand-based. This result is consistent with the fact that the UV–vis spectrum of **3** is not significantly different from that of the free ligand. This comparison also highlights the role of the disilver core of **2** and **4** with respect to generating the observed MMLCT transitions: the silver–silver interaction raises the energy of the silver-based orbitals in the dimeric complexes.

Extensive theoretical studies since the 1980s have probed the potential bonding between closed-shell metal centers with metallophilic interactions.[5b] A first-level analysis indicates that d^8 and d^{10} configurations lead to both metal–metal bonding and antibonding molecular orbitals being fully occupied, producing a bond order of zero.[7,17] More subtle effects, however, such as symmetry-allowed mixing of metal s, p, and d orbitals, have been shown in several cases to result in a net weak bonding interaction.[18] For both complexes **2** and **4**, the calculated Mayer bond order between the two silver centers is 0.13,[19] a value consistent with previously reported calculations for closed-shell metallophilic interactions.[20] Thus, the increased orbital overlap for the silver centers in **2**, as compared to **4**, does not lead to an increased bond order, because both the silver–silver bonding and antibonding MOs are fully occupied. Attempts to oxidize complex **2**, in order to remove electrons from the $\sigma^*_{\mathrm{Ag-Ag}}$ HOMO and thereby promote increased silver–silver bonding, have led only to ill-defined product mixtures. We speculate that facile ligand scrambling (such as observed for the interconversion between **2** and **4**) likely contributes to our inability to cleanly oxidize **2**.

Photophysical Properties. Molecules and materials with silver–silver interactions have long been investigated for their optical properties, including photoluminescent behavior.[3] However, the visible region MMLCT transitions displayed by complexes **2** and **4** are unique among silver(I) dimers. To better understand these complexes' photophysical properties, we examined both their emission spectra and their transient absorption (TA) spectra. These measurements were performed on anhydrous, argon-saturated solutions of **2** and **4·PF$_6$**, conditions in which the solution-phase structures of both complexes are well-defined (*vide supra*).

Transient absorption obtained by laser flash photolysis (LFP) of **2** in CH_2Cl_2 solution was both broad and weak between 400 and 600 nm, with a peak near 500 nm (Figure 6, top). The TA spectrum is accompanied by a bleach between 360–390 nm. This bleach, which corresponds to loss of the starting material, suggests that the transient species is formed directly from the ground state of **2** without prior intermediates. The kinetics for this solution showed a monoexponential decay fit with a rate constant of $7.5 \times 10^5 \pm 0.8 \times 10^5$ s^{-1} and thus a lifetime of 1.3 μs (Figure S6). The transient absorption feature around 500 nm is consistent with the absorption profile of the ^{i}PrNDI ligand in its radical anion form,[14a] which supports the assignment of MMLCT character in the excited state of **2**, as predicted by TD-DFT calculations.

The TA spectra obtained by LFP of complex **4·PF$_6$** show significantly stronger absorbance as compared to complex **2**, but a similar broad feature spanning approximately 400–600 nm (Figure 6, bottom). The kinetics for the decay of this species were fit with a monoexponential curve, yielding a rate constant of $1.27 \times 10^6 \pm 0.03 \times 10^6$ s^{-1} and a lifetime of 788 ns (Figure S7), which is about half the lifetime measured for compound **2**. For comparison, LFP of ligand **1** in CH_2Cl_2 solutions did not produce any observable transient absorption features on the time scale of our measurements.[21] The relatively long excited state lifetimes observed here for compounds **2** and **4** are noteworthy because they compare favorably to metal dimers with charge transfer excited states that have recently been studied for their visible light absorption and excited state reactivity, using precious metals such as rhodium and platinum.[10]

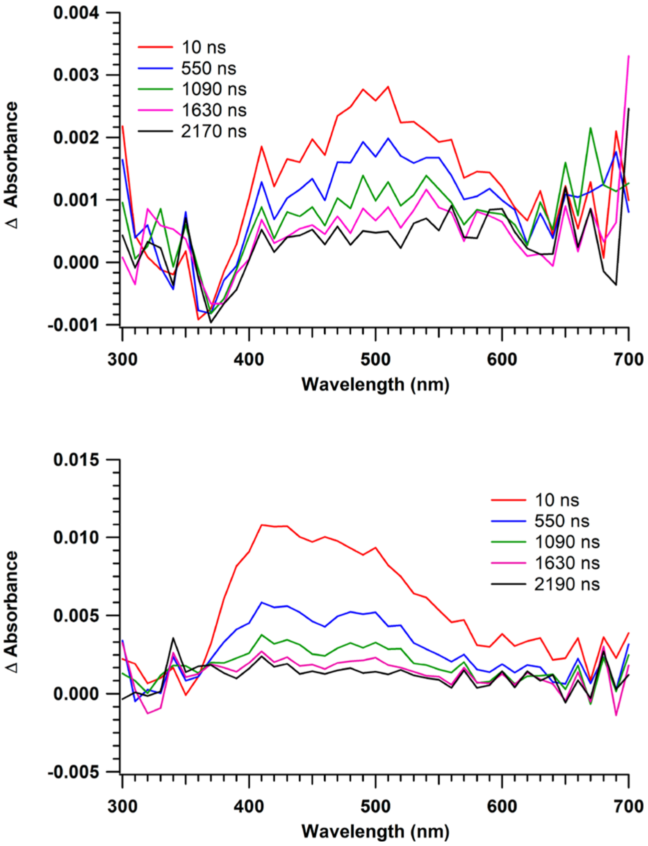

Figure 6. Transient absorption spectra obtained by LFP (λ_{ex} = 355 nm) of argon-saturated CH_2Cl_2 solutions of **2** (top) and **4·PF$_6$** (bottom).

In order to further probe the nature of the excited states of compounds **2** and **4**, fluorescence and phosphorescence measurements were also undertaken. The results of solution fluorescence conducted in argon-saturated CH_2Cl_2 solutions using 355 nm excitation are shown in the top panel of Figure 7. Compound **4** clearly shows a higher fluorescence emission than compound **2**, exhibiting a large emission peak at 400 nm. In contrast, compound **2** shows broad and weak fluorescence ranging from 360 to 550 nm. Phosphorescence spectra, collected at 77 K in a glassy matrix of 1:1 CH_2Cl_2:toluene, help to account for the disparity in the fluorescence emission spectra (Figure 7, bottom). While compound **4** shows negligible phosphorescence above baseline noise, compound **2** shows a weak, but appreciable, phosphorescence signature centered at approximately 700 nm. From these data, it is possible that compound **2** has an easier path to intersystem crossing than compound **4**, which could account for the lower fluorescence emission observed for compound **2**. The lack of phosphorescence for complex **4** could indicate that its path to intersystem crossing is very slow or inaccessible, though we note that other fast nonradiative processes are also possible.

■ CONCLUSIONS

Here we have described the synthesis and characterization of two new dinuclear silver(I) complexes that feature a redox-active naphthyridine diimine ligand. For both complexes, the disilver core, in combination with low-lying ligand π^* orbitals, produces transitions with MMLCT character in the visible region. Characterization of the MMLCT excited states revealed surprisingly long lifetimes on the order of 1 μs. Furthermore, structural differences between the two complexes lead to appreciable differences in their photophysical properties, as revealed by their emission spectra. These results suggest that silver(I) dimers with redox-active ligands may hold promise as tunable chromophores for applications in visible light photochemistry, which represents a previously unexplored area of research for silver.

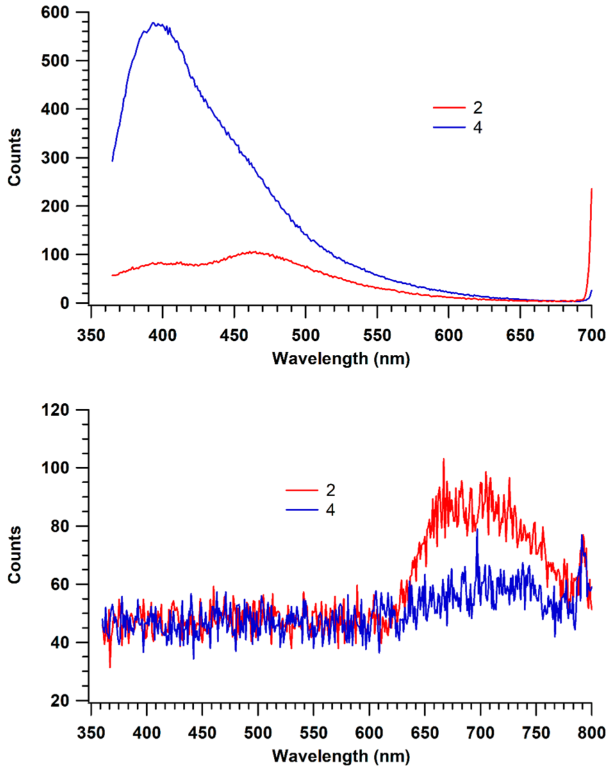

Figure 7. (top) Fluorescence spectra of compounds **2** and **4·PF$_6$** in argon-saturated CH_2Cl_2 solutions at room temperature (λ_{ex} = 355 nm). (bottom) Phosphorescence spectra of compounds **2** and **4·PF$_6$** in a glassy 1:1 CH_2Cl_2:toluene matrix at 77 K (λ_{ex} = 355 nm).

■ ASSOCIATED CONTENT

Supporting Information

The Supporting Information is available free of charge at https://pubs.acs.org/doi/10.1021/acs.inorgchem.0c02938.

Experimental procedures, spectroscopic data, and crystallographic data (PDF)

Accession Codes

CCDC 1997402–1997404 and 2022245 contain the supplementary crystallographic data for this paper. These data can be obtained free of charge via www.ccdc.cam.ac.uk/data_request/cif, or by emailing data_request@ccdc.cam.ac.uk, or by contacting The Cambridge Crystallographic Data Centre, 12 Union Road, Cambridge CB2 1EZ, UK; fax: +44 1223 336033.

■ AUTHOR INFORMATION

Corresponding Author

Michael G. Campbell − *Department of Chemistry, Barnard College, New York, New York 10027, United States;* orcid.org/0000-0002-4174-0174; Email: mcampbel@barnard.edu

Authors

Dylan J. Shields − *Department of Chemistry, University of Cincinnati, Cincinnati, Ohio 45221, United States*

Tasneem Elkoush − *Department of Chemistry, Barnard College, New York, New York 10027, United States*

Emily Miura-Stempel − *Department of Chemistry, Barnard College, New York, New York 10027, United States*

Choi L. Mak − *Department of Chemistry, Barnard College, New York, New York 10027, United States*

Guang-Hao Niu − *Department of Chemistry, Barnard College, New York, New York 10027, United States*

Anna D. Gudmundsdottir − *Department of Chemistry, University of Cincinnati, Cincinnati, Ohio 45221, United States*

Complete contact information is available at:
https://pubs.acs.org/10.1021/acs.inorgchem.0c02938

Notes

The authors declare no competing financial interest.

■ ACKNOWLEDGMENTS

We thank Brandon Fowler for assistance with HRMS data collection. M.G.C. gratefully acknowledges the ACS PRF (59369-UNI3) and the NSF (CHE-1956197) for financial support, and the NSF (CHE-1827936) for an MRI award in support of a 400 MHz NMR spectrometer at Barnard College. T.E., E.M.-S., C.L.M., and M.G.C. thank the Department of Chemistry and the Office of the Provost at Barnard College for additional financial support. A.D.G. and D.J.S. thank NSF (CHE-1800140) and OSC (PES0597). D.J.S. acknowledges Doctoral Enhancement Fellowships, an Ann P. Villalobos/Laws Fellowship. SCXRD data were collected at the Shared Materials Characterization Laboratory at Columbia University.

■ REFERENCES

(1) (a) Cui, Y.; He, C. Efficient Aziridination of Olefins Catalyzed by a Unique Disilver(I) Compound. *J. Am. Chem. Soc.* **2003**, *125*, 16202−16203. (b) Li, Z.; Capretto, D. A.; Rahaman, R.; He, C. Silver-Catalyzed Intermolecular Amination of C−H Groups. *Angew. Chem., Int. Ed.* **2007**, *46*, 5184−5186. (c) Safin, D. A.; Pialat, A.; Korobkov, I.; Murugesu, M. Unprecedented Trinuclear Ag(I) Complex with 2,4,6-Tris(2-pyrimidyl)-1,3,5-triazine as an Efficient Catalyst for the Aziridination of Olefins. *Chem. - Eur. J.* **2015**, *21*, 6144−6149.

(2) (a) Khlobystov, A. N.; Blake, A. J.; Champness, N. R.; Lemenovskii, D. A.; Majouga, A. G.; Zyk, N. V.; Schröder, M. Supramolecular design of one-dimensional coordination polymers based on silver(I) complexes of aromatic nitrogen-donor ligands. *Coord. Chem. Rev.* **2001**, *222*, 155−192. (b) Chen, C.-L.; Kang, B.-S.; Su, C.-Y. Recent Advances in Supramolecular Design and Assembly of Silver(I) Coordination Polymers. *Aust. J. Chem.* **2006**, *59*, 3−18. (c) Zhang, T.; Ji, C.; Wang, K.; Hu, D.; Meng, X.; Chen, C. One-dimensional coordination polymer and its hydrogen bonded 2D network generated from dimeric Ag(I) building units. *Inorg. Chim. Acta* **2007**, *360*, 1609−1615.

(3) (a) Tong, M.-L.; Chen, X.-M.; Ye, B.-H.; Ji, J.-N. Self-Assembled Three-Dimensional Coordination Polymers with Unusual Ligand-Unsupported Ag−Ag Bonds: Synthesis, Structures, and Luminescent Properties. *Angew. Chem., Int. Ed.* **1999**, *38*, 2237−2240. (b) Sun, D.; Cao, R.; Weng, J.; Hong, M.; Liang, Y. A novel luminescent 3D polymer containing silver chains formed by ligand unsupported Ag−Ag interactions and organic spacers. *J. Chem. Soc., Dalton Trans.* **2002**, 291−292. (c) Che, C.-M.; Tse, M.-C.; Chan, M. C. W.; Cheung, K.-K.; Phillips, D. L.; Leung, K.-H. Spectroscopic Evidence for Argentophilicity in Structurally Characterized Luminescent Binuclear Silver(I) Complexes. *J. Am. Chem. Soc.* **2000**, *122*, 2464−2468.

(4) (a) Zheng, S.-L.; Zhang, J.-P.; Wong, W.-T.; Chen, X.-M. A Novel, Highly Electrical Conducting, Single-Component Molecular Material: $[Ag_2(ophen)_2]$ (Hophen = 1*H*-[1,10]phenanthroline-2-one). *J. Am. Chem. Soc.* **2003**, *125*, 6882−6883. (b) Lin, P.; Henderson, R. A.; Harrington, R. W.; Clegg, W.; Wu, C.-D.; Wu, X.-T. New 1- and 2-Dimensional Polymeric Structures of Cyanopyridine Complexes of Ag^I and Cu^I. *Inorg. Chem.* **2004**, *43*, 181−188.

(5) (a) Jansen, M. Homoatomic d^{10}−d^{10} Interactions: Their Effects on Structure and Chemical and Physical Properties. *Angew. Chem., Int. Ed. Engl.* **1987**, *26*, 1098−1110. (b) Pyykkö, P. Strong Closed-Shell Interactions in Inorganic Chemistry. *Chem. Rev.* **1997**, *97*, 597−636.

(6) Schmidbaur, H.; Schier, A. Argentophilic Interactions. *Angew. Chem., Int. Ed.* **2015**, *54*, 746−784.

(7) *Multiple Bonds Between Metal Atoms*, 3rd ed.; Cotton, F. A., Murillo, C. A., Walton, R. A., Eds.; Springer: Boston, MA, 2005.

(8) (a) Mak, C. L.; Bostick, B. C.; Yassin, N. M.; Campbell, M. G. Argentophilic Interactions in Solution: An EXAFS Study of Silver(I) Nitrene Transfer Catalysts. *Inorg. Chem.* **2018**, *57*, 5720−5722. (b) Elkoush, T.; Mak, C. L.; Paley, D. W.; Campbell, M. G. Silver(II) and Silver(III) Intermediates in Alkene Aziridination with a Dinuclear Silver(I) Nitrene Transfer Catalyst. *ACS Catal.* **2020**, *10*, 4820−4826.

(9) Thompson, D. W.; Ito, A.; Meyer, T. J. $[Ru(bpy)_3]^{2+*}$ and other remarkable metal-to-ligand charge transfer (MLCT) excited states. *Pure Appl. Chem.* **2013**, *85*, 1257−1305.

(10) (a) Whittemore, T. J.; Sayre, H. J.; Xue, C.; White, T. A.; Gallucci, J. C.; Turro, C. New Rh_2(II,II) Complexes for Solar Energy Applications: Panchromatic Absorption and Excited-State Reactivity. *J. Am. Chem. Soc.* **2017**, *139*, 14724−14732. (b) Whittemore, T. J.; Millet, A.; Sayre, H. J.; Xue, C.; Dolinar, B. S.; White, E. G.; Dunbar, K. R.; Turro, C. Tunable Rh_2(II,II) Light Absorbers as Excited-State Electron Donors and Acceptors Accessible with Red/Near-Infrared Irradiation. *J. Am. Chem. Soc.* **2018**, *140*, 5161−5170. (c) Sayre, H. J.; Millet, A.; Dunbar, K. R.; Turro, C. Photocatalytic H_2 production by dirhodium(II,II) photosensitizers with red light. *Chem. Commun.* **2018**, *54*, 8332−8334. (d) Chakraborty, A.; Yarnell, J. E.; Sommer, R. D.; Roy, S.; Castellano, F. N. Excited-State Processes of Cyclometallated Platinum(II) Charge-Transfer Dimers Bridged by Hydroxypyridines. *Inorg. Chem.* **2018**, *57*, 1298−1310. (e) Yang, H.-M.; Liu, M.-L.; Tu, J.-W.; Miura-Stempel, E.; Campbell, M. G.; Chuang, G. J. Bimetallic Photoredox Catalysis: Visible Light-Promoted Aerobic Hydroxylation of Arylboronic Acids with a Dirhodium(II) Catalyst. *J. Org. Chem.* **2020**, *85*, 2040−2047.

(11) (a) Gavrilova, A. L.; Bosnich, B. Principles of Mononucleating and Binucleating Ligand Design. *Chem. Rev.* **2004**, *104*, 349−383. (b) Bera, J. K.; Sadhukhan, N.; Majumdar, M. 1,8-Naphthyridine Revisited: Applications in Dimetal Chemistry. *Eur. J. Inorg. Chem.* **2009**, *2009*, 4023−4038.

(12) (a) Munakata, M.; Maekawa, M.; Kitagawa, S.; Adachi, M.; Masuda, H. Synthesis, Properties and Crystal Structures of Dicopper(I) and Disilver(I) Complexes with 1,8-naphthyridine (napy): $[Cu_2(napy)_2](ClO_4)_2$ and$[Ag_2(napy)_2](ClO_4)_2$. *Inorg. Chim. Acta* **1990**, *167*, 181−188. (b) Koizumi, T.; Tanaka, K. Synthesis and crystal structures of mono- and dinuclear silver(I) complexes bearing 1,8-naphthyridine ligand. *Inorg. Chim. Acta* **2004**, *357*, 3666−3672. (c) Jin, S.-W.; Chen, W.-Z.; Wang, D.-Q. Synthesis and Structural Characterization of Mononuclear and Dinuclear Silver Complexes of Naphthyridinone. *Chin. J. Inorg. Chem.* **2007**, *23*, 270−274. (d) Giordana, A.; Priola, E.; Bonometti, E.; Benzi, P.; Operti, L.; Diana, E. Structural and spectroscopic study of the asymmetric 2-(2′-pyridyl)-1,8-naphthyridine ligand with closed-shell metals. *Polyhedron* **2017**, *138*, 239−248.

(13) Niu, G.-H.; Wentz, H. C.; Zheng, S.-L.; Campbell, M. G. Silver(I) coordination polymers from dinucleating naphthyridine ligands. *Inorg. Chem. Commun.* **2019**, *101*, 142−144.

(14) (a) Zhou, Y.-Y.; Hartline, D. R.; Steiman, T. J.; Fanwick, P. E.; Uyeda, C. Dinuclear Nickel Complexes in Five States of Oxidation Using a Redox-Active Ligand. *Inorg. Chem.* **2014**, *53*, 11770−11777.

(b) Uyeda, C.; Steiman, T. J.; Pal, S. Catalytically Active Nickel−Nickel Bonds Using Redox-Active Ligands. *Synlett* **2016**, *27*, 814−820. (c) Zhou, Y.-Y.; Uyeda, C. Catalytic reductive [4 + 1]-cycloadditions of vinylidenes and dienes. *Science* **2019**, *363*, 857−862.

(15) (a) Ziessel, R.; Harriman, A.; El-ghayoury, A.; Douce, L.; Leize, E.; Nierengarten, H.; Van Dorsselaer, A. First assembly of copper(I) naphthyridine-based helicates. *New J. Chem.* **2000**, *24*, 729−732. (b) Dutta, I.; Sarbajna, A.; Pandey, P.; Rahaman, S. M. W.; Singh, K.; Bera, J. K. Acceptorless Dehydrogenation of Alcohols on a Diruthenium(II,II) Platform. *Organometallics* **2016**, *35*, 1505−1513.

(16) (a) Jurca, T.; Gorelsky, S. I.; Korobkov, I.; Richeson, D. S. Novel pincer complexes of Ag(I), coordination of toluene and their comparison with indium analogues. *Dalton Trans.* **2011**, *40*, 4394−4396. (b) Jurca, T.; Ouanounou, S.; Gorelsky, S.; Korobkov, I.; Richeson, D. S. The interplay of metal and supporting ligand in labile coordination to pincer complexes of Ag(I). *Dalton Trans.* **2012**, *41*, 4765−4771.

(17) Cotton, F. A.; Feng, X.; Matusz, M.; Poli, R. Experimental and Theoretical Studies of the Copper(I) and Silver(I) Dinuclear *N,N′*-Di-*p*-tolylformamidinato Complexes. *J. Am. Chem. Soc.* **1988**, *110*, 7077−7083.

(18) (a) Mann, K. R.; Lewis, N. S.; Williams, R. M.; Gray, H. B.; Gordon, J. G. Further studies of metal-metal bonded oligomers of rhodium(I) isocyanide complexes. Crystal structure analysis of octakis(phenylisocyanide)dirhodium bis(tetraphenylborate). *Inorg. Chem.* **1978**, *17*, 828−834. (b) Merz, K. M.; Hoffmann, R. d^{10}−d^{10} Interactions: Multinuclear Copper(I) Complexes. *Inorg. Chem.* **1988**, *27*, 2120−2127.

(19) Bridgeman, A. J.; Cavigliasso, G.; Ireland, L. R.; Rothery, J. The Mayer bond order as a tool in inorganic chemistry. *J. Chem. Soc., Dalton Trans.* **2001**, 2095−2108.

(20) (a) Zheng, S.-L.; Nygren, C. L.; Messerschmidt, M.; Coppens, P. Ligand-unsupported Au(I) chains with short Au(I)···Au(I) contacts. *Chem. Commun.* **2006**, 3711−3713. (b) Bercaw, J. E.; Durrell, A. C.; Gray, H. B.; Green, J. C.; Hazari, N.; Labinger, J. A.; Winkler, J. A. Electronic Structures of Pd^{II} Dimers. *Inorg. Chem.* **2010**, *49*, 1801−1810.

(21) This observation is consistent with previously reported studies on naphthyridine-based small organic molecules: Boldridge, D. W.; Scott, G. W. Excited singlet state absorption spectra and relaxation kinetics of the azanaphthalenes. *J. Chem. Phys.* **1986**, *84*, 6790−6798.